ChemComm

Highly conductive, flexible and scalable graphene hybrid thin films with controlled domain size as transparent electrodes

Journal:	*ChemComm*
Manuscript ID:	CC-COM-02-2014-001302.R1
Article Type:	Communication
Date Submitted by the Author:	31-Mar-2014
Complete List of Authors:	Jang, Jyongsik; Seoul National University, Shin, Keun-Young; Seoul National University, School of Chemical and Biological Engineering

Cite this: DOI: 10.1039/coxx00000x

www.rsc.org/chemcomm

COMMUNICATION

Highly conductive, flexible and scalable graphene hybrid thin films with controlled domain size as transparent electrodes

Keun-Young Shin and Jyongsik Jang*

Received (in XXX, XXX) Xth XXXXXXXXX 200X, Accepted Xth XXXXXXXXX 200X
DOI: 10.1039/b000000x

Highly conductive, transparent, flexible and scalable graphene hybrid thin films with controlled domain size was successfully fabricated via mechanochemical method, screen printing and pressure-assisted reduction process.

Graphene has emerged to be a transparent conductive material for various optoelectronic and photovoltaic devices due to its excellent mechanical strength with flexibility, high transmittance, and outstanding electron mobility.[1] Especially, reduced graphene oxide (rGO), derived chemically from natural graphite via oxidative exfoliation and subsequent reduction, has attracted a great deal of interest because of its solution processability, high volume production at low cost, and the simplicity of the fabrication technique.[2] However, it had fundamental limitations in conductivity originated from the large number of unreduced oxygen-containing functional groups and intersheet junctions between the graphene domains.[3]

In order to improve the recovery in the electrical conductivity, high-temperature annealing is highly desirable, which is time-consuming and complicated.[4] Therefore, we have previously reported on the fabrication of rGO transparent electrodes via the pressure-assisted reduction at relatively mild temperature, which was applicable to use flexible substrates.[5] Furthermore, for the enhancement of connectivity between the graphene sheets, several methods have been introduced such as synthesis of ultra-large size rGO sheets, blending with other conducting materials including carbon nanotube, Ag nanowire and conducting polymer, and doping with metal nanoparticles as an electron donor.[6] In spite of recent advances in the reduction of vacant lattice sites, it is still challenging to easily fabricate the highly conductive and large-area graphene thin film with uniformity.[7]

Herein, we report a novel and simple route for the fabrication of highly conductive and flexible graphene thin films in the large-scale via screen printing and pressure-assisted reduction process for transparent electrodes. To the best of our knowledge, this is the first attempt of utilizing graphene hybrid thin films with controlled domain size, which are derived from the mechanochemical method. Importantly, as a connecting bridge, submicrometer-sized graphene sheets increased the dispersibility and the interfacial interactions between graphene sheets with micrometer size, which caused the increase in conductivity related to the high reduction efficiency. In addition, our results demonstrated that the graphene hybrid thin films exhibited uniform conductivity and outstanding flexibility.

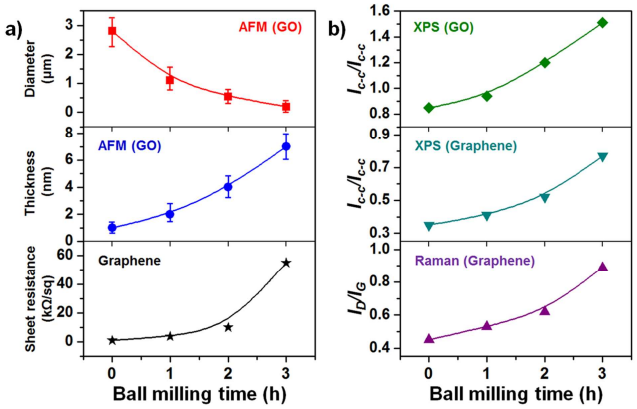

Fig. 1 Properties and structure variation of size-controlled GO and graphene as a function of ball milling time. Size and thickness were detected by AFM analysis, and peak intensity ratios of the C−O to C−C and the D to G were obtained from XPS and Raman spectra, respectively. Electrical sheet resistance was measured with a four-point probe.

The properties and structure variation of size-controlled GO and graphene as a fuction of ball milling time are shown in Fig. 1 (ESI†). Generally, the graphite's carbon atoms (~20 μm) positioned in adjacent planes are bound by weak interplanar forces, which make it possible to have submicrometer-size via mechanical ball milling process.[8] Furthermore, the size of graphite could be easily controlled by ball milling time, and three types of ball (1, 2, and 5 mm) were used for effective ball milling process (ESI†). In our study, size-controlled GO was synthesized from ball-milled graphite by chemical exfoliation, and it was used as a conducing ink for screen printing. The reduction process for graphene sheets was performed by mild thermal annealing with hydrazine vapor deposition and pressure-assisted heat treatment using hot press.[9] As a result of the mechanochemical method, the diameter of GO sheet highly reduced (200−300 nm), whereas the thickness gradually increased (4−10 nm) (Fig. 1a). Interestingly, the morphology has been transformed from flake to spherical form, which inidicated of surface grinding by high mechanical energy (ESI†). To gain more insight into the size-controlled GO and graphene property, XPS and Raman analysis were conducted (Fig. 1b). The result was that I_{C-O}/I_{C-C} ratios of 0h and 3h ball-milled GO decreased from 0.85 and 1.51 to 0.35 and 0.77 via reduction process, respectively. Moreover, the Raman spectrum indicated an increased I_D/I_G intensity ratio and reduced 2D peak intensity. The increased defects can be attributed to the structural edge

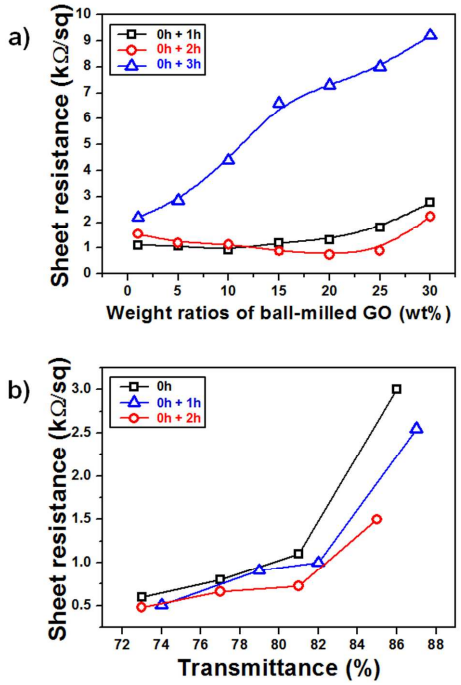

Fig. 2 Sheet resistance of graphene hybrid thin film as a function of (a) ball-milled GO concentration and (b) transmittance. Film transmittance was controlled by adjusting the number of screen-printing steps. Pristine graphene thin film (0h) was fabricated via two step reduction process of pristine GO thin film.

effects from the average size reduction of the sp^2 domains. Namely, active sites of ball-milled GO sheets with small domain size could afford to bind more oxygen functional groups on basal and edge planes due to their high surface area. For this reason, ball-milled graphene sheets had low conductivity comparing to non-milled graphene sheets.

In order to investigate the size confinement effect to electrical property of graphene sheets for transparent conductive electrode, graphene hybrid thin films with controlled domain size were fabricated on PES film according to the weight content of size-controlled graphene under same transmittance of 81% (Fig. 2a). As a result, it was noteworthy that the hybrid thin film with 20 wt% of 2h ball-milled graphene had a low sheet resistance of 0.73 kΩ sq^{-1}. This is *ca.* 1.5 times lower than the sheet resistance of pristine graphene thin film, thus suggesting a bridging effect of small domain-sized graphene (400−700 nm) between adjacent graphene layers with micometer size along the horizontal and vertical axes. In the case of 1h ball-milled graphene, the sheet resistance has been minimized at 10 wt%. As the concentration increased to over optimum point, the conductivity of graphene hybrid thin film decreased. In particular, when the 3h ball-milled graphene was mixed in graphene hybrid film, this phenomena has disappeared due to its very small domain size and low conductivity, which is insufficient to play a connection role. Furthermore, the fine tuning of the surface sheet resistance and transmittance was accomplished by controlling the number of screen printing (Fig. 2b). Overally, the transmittance and sheet resistance of graphene hybrid thin films have decreased as increased printing steps. Especially, the graphene hybrid thin films with 2h ball-milled graphene had sheet resistances of 0.49, 0.66 and 1.51 kΩ sq^{-1} at room temperature and transmittance (550 nm wavelength) of 73.25, 77.58 and 85.65 %, respectively.

To achieve an in-depth insight into the bridging effect by controlled domain size of graphene sheet, 3D atomic force microscopy (AFM) analysis of graphene hybrid thin film with 2h ball-milled graphene was conducted in comparision with that of pristine graphene thin film (Fig. 3a and b). As a result, it was proved that graphene hybrid thin film consisted of micrometer and submicrometer-sized graphene sheets. Most of all, the vacant lattice sites in the pristine graphene sheets have been filled with submicrometer-sized graphene sheets, which caused the short electron transport pathway. Dynamic light scattering (DLS) analysis also shows that GO hybrid solution has various peak diameter with dense size distribution relative to pristine GO solution, which demonstrates a mixed domain size (Fig. 3c and d). In addition, GO hybrid solution exhibited a superior sedimentation ratio compared to that of pristine GO solution, and there is no sediment deposited after ninety days (Fig. 3e). This superb dispersion stability can be ascribed in terms of the sedimentation velocity (V_g), which is a significant factor in particle precipitation.[10] According to the Stoke's equation, values were 2.375 × 10^{-7} and 8.825 × 10^{-9} m s^{-1} for pristine GO and hybrid GO solution, respectively (ESI†). It means that the V_g value of GO hybrid sheet is *ca.* 27 times slower than that of pristine GO sheet. It is also expected that the small domain size and high oxygen functional groups would have a combined or

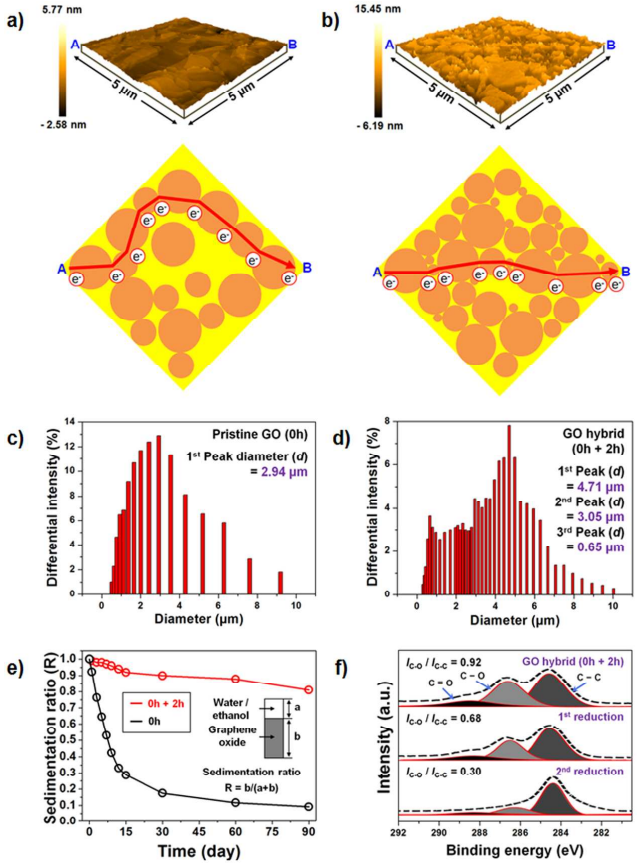

Fig. 3 The 3D AFM images and schematic illustration showing electron pathway of (a) pristine graphene and (b) graphene hybrid thin film. (c and d) DLS analysis and (e) sedimentation properties of pristine GO and GO hybrid solution (inset: definition of sedimentation ratio). (f) XPS spectrum of GO and graphene hybrid film via two step reduction process.

synergistic effect on the enhancement in anti-sedimentation property. Therefore, these filled domain property and outstanding dispersibility could lead to high reduction efficiency and low I_{C-O}/I_{C-C} ratio under pressure-assisted heat treatment (Fig. 3f). In other words, sufficient thermal energy by direct contact can be effectively trasferred to dissociate functional groups from GO hybrid thin film, minimizing the number of voids and maximizing the area of heat flow.

To assess the uniformity and flexibility, the pristine and graphene hybrid thin film with a 15-cm square pattern were fabricated via screen printing. The sheet resistance change is expressed as $\Delta R/R_s = (R-R_s)/R_s$, where R and R_s are the measured and initial average sheet resistance, respectively. Fig. 4a shows that the graphene hybrid thin film had good interplanar electrical contact between the graphene sheets over about 14% of the sheet resistance distribution, compared to a 38% for pristine graphene thin film. Furthermore, electrical fatigue tests were performed using an external force. The overall sheet resistance increased in proportion to the folding angle (Fig. 4b). Folding the hybrid thin film −180° (acute angle) and +180° (obtuse angle) led to approximately 10 and 12.5 % increases in sheet resistance, respectively. In the case of pristine graphene thin film, increased values were *ca.* 15.6 and 17.4 %, respectively, which indicated of high electrical fatigue damage. In addition, when the samples were released from bending after 500 cycles, R value of the pristine graphene and hybrid thin films increased by *ca.* 3.9 and 1.27 kΩ sq^{-1}, respectively (Fig. 4c). This indicates a high degree of structural stability in the graphene hybrid thin film. Judging from these result, it was evident that domain size-controlled graphene acted as a bridge connecting graphene with micrometer size, and enhanced the interfacial interactions between graphene sheets. Moreover, outstanding dispersibility could make it possible to have improved adhesion of the graphene hybrid thin film to the flexible PES substrate.

In conclusion, a graphene hybrid thin film with controlled domain size was successfully fabricated via mechanochemical method and screen printing. Most of all, large-area graphene hybrid thin film with uniformity and flexibility would be suitable for use as a commercial transparent conductive electrode.

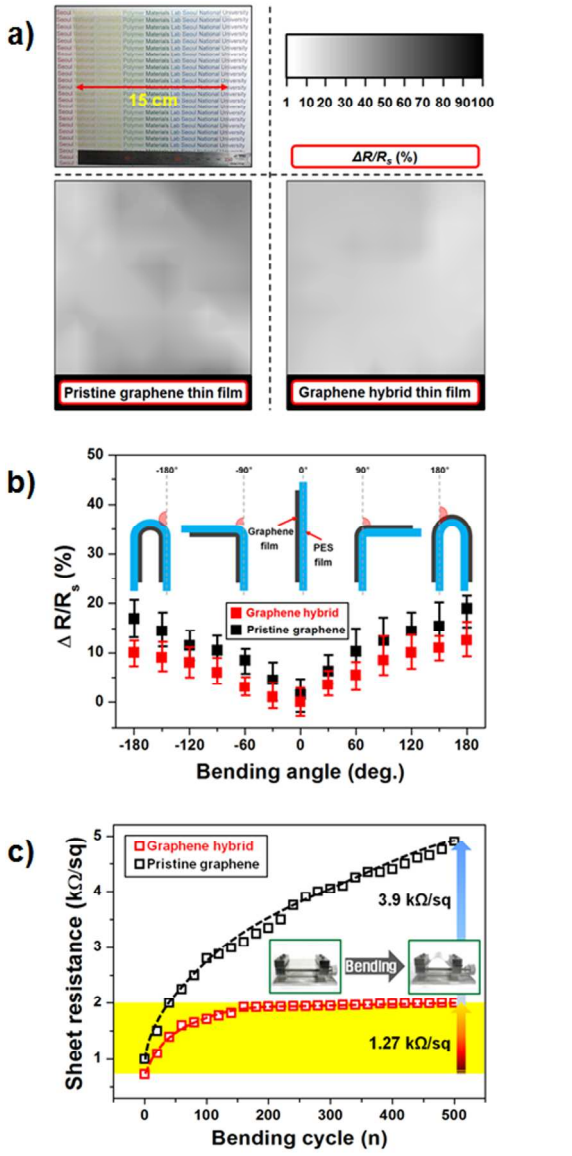

Fig. 4 (a) Distribution of sheet resistance for pristine graphene and graphene hybrid thin film for a 15-cm square pattern. Sheet resistance changes of pristine graphene and graphene hybrid thin film according to the bending (b) angle and (c) cycle. Inset in (b): schematic diagram of folded film on PES substrate under tensile or compressive strain.

Notes and references

World Class University (WCU) program of Chemical Convergence for Energy & Environment (C_2E_2), School of Chemical and Biological Engineering, College of Engineering, Seoul National University (SNU), Seoul, Korea. Fax: 82 2 888 1604; Tel: 82 2 880 7069; E-mail: jsjang@plaza.snu.ac.kr

† Electronic Supplementary Information (ESI) available: [experimental section, schematic illustration and SEM images for size-controlled graphite, AFM images, XPS spectrum, and Raman sprectra of size-controlled GO and graphene, and Stoke's law]. See DOI: 10.1039/b00000x/

1 (a) K.-Y. Shin, J.-Y. Hong, J. Jang, *Chem. Commun.* 2011, 47, 8527; (b) D. Li , M. B. Muller, S. Gilke, R. B. Kaner, G. G. Wallace, *Nat. Nanotechnol.* 2008, 3, 101; (c) W. Yuan, A. Liu, L. Huang, C. Li, G. Shi, *Adv. Mater.* 2013, 25, 766.

2 (a) G. Eda, M. Chhowalla, *Adv. Mater.* 2010, 22, 2392; (b) D. R. Dreyer, S. Park, C. W. Bielawski, R. S. Ruoff, *Chem. Soc. Rev.* 2010, 39, 228.

3 (a) M. S. Kang, K. T. Kim, J. U. Lee, W. H. Jo, *J. Mater. Chem. C* 2013, 1, 1870; (b) J. Zhao, S. Pei, W. Ren, L. Gao, H.-M. Cheng, *ACS Nano* 2010, 4, 5245.

4 (a) H. A. Becerril, J. Mao, Z. Liu, R. M. Stoltenberg, Z. Bao, Y. Chen, *ACS Nano* 2008, 2, 463; (b) Z. S. Wu, W. C. Ren, L. B. Gao, B. L. Liu, C. B. Jiang, H. M. Cheng, *Carbon* 2009, 47, 493.

5 (a) K.-H. Shin, Y. Jang, B.-S. Kim, J. Jang, S. H. Kim, *Chem. Commun.* 2013, 49, 4887.

6 (a) X. Lin, X. Shen, Q. B. Zheng, N. Youse, L. Ye, Y. W. Mai, J. K. Kim, *ACS Nano* 2012, 6, 10708; (b) K.-Y. Shin, S. Cho, J. Jang, *small* 2013, 9, 3792; (c) H. Chang, H. Wu, *Adv. Funct. Mater.* 2013, 23, 1984; (d) C. Y. Li, Z. Li, H. W. Zhu, K. L. Wang, J. Q. Wei, X. A. Li, *J. Phys. Chem. C* 2010, 114, 14008; (e) K. K. Kim, A. Reina, Y. Shi, H. Park, L. J. Li, Y. H. Lee, J. Kong, *Nanotechnology* 2010, 21, 285205.

7 (a) X. Z. Tang, Z. W. Cao, H. B. Zhang, J. Liu, Z. Z. Yu, *Chem. Commun.* 2011, 47, 3084; (b) B.-T. Liu, H.-L. Kuo, *Carbon* 2013, 63, 390.

8 (a) K.-Y. Shin, J.-Y. Hong, S. Lee, J. Jang, *J. Mater. Chem.* 2012, 22, 23404; (b) Q. Tang, J. Wu, Q. Li, J. Lin, *Polymer* 2008, 49, 5329.

9 (a) N. J. Welham, V. Berbenni, P. G. Chapman, *J. Alloys Compd.* 2003, 349, 255; (b) W. Duan, *Appl. Mech. Mater.* 2011, 80, 229; (c) K.-Y. Shin, J.-Y. Hong, J. Jang, *Adv. Mater.* 2011, 23, 2113; (d) W. S. Hummers, R. E. Offeman, *J. Am. Chem. Soc.* 1958, 80, 1339.

10 (a) H. Yilmaz, U. Yilmaz, *J. Appl. Polym. Sci.* 2007, 103, 3798; (b) J.-Y. Hong, J. Jang, *Soft Matter* 2012, 8, 3348.